International Journal of Innovative Computing, Information and Control
Volume **12**, Number **2**, April **2016**

ICIC International ©2016 ISSN 1349-4198
pp. 557–568

A METHOD FOR W-BAND DOPPLER RADAR BASED IN-BORE PROJECTILE MEASUREMENT PARAMETERS EXTRACTION

Li Wu[1], Limei Wang[2], Xuan Lu[1] and Shusheng Peng[1]

[1]School of Electronic and Optical Engineering
Nanjing University of Science and Technology
No. 200, Xiaolingwei Street, Xuanwu District, Nanjing 210094, P. R. China
li_wu@njust.edu.cn; nanliluxuan@126.com; njustpss@163.com

[2]Anhui Sun Create Electronics Corp.
Camphor Avenue 199, National High-Tech Industrial Development Zone, Hefei 230088, P. R. China
wanglimeimoon@126.com

Received August 2015; revised December 2015

Abstract. *It is critical in ballistic studies to achieve accurate and continuous measurements of the motion parameters for in-bore projectile. This paper presents a signal processing method for W-band Doppler radar based in-bore projectile monitoring with the time-frequency analysis and digital image processing combined techniques. Firstly, a concentration measure based improved time-frequency peak filtering (ITFPF) method is presented as a pre-processing step to reduce noise. Next a time-frequency image ridge extraction and optimization method is proposed based on the curvilinear structure detection and mathematical morphology (MM). Finally, least square fitting is employed to fit the optimized time-frequency ridge point set with a polynomial function, with which the instantaneous frequency (IF) of the signal is estimated. Thus, the motion parameters of the in-bore projectile could be correspondingly extracted. The presented simulation and experiment results demonstrate the effectiveness and accuracy of the presented method.*
Keywords: Time-frequency peak filtering, Image processing, Instantaneous frequency estimation, Projectile parameters measurement

1. **Introduction.** It is critical to obtain accurate and continuous measurements of the motion parameters for in-bore projectile in areas of artillery design, development and production. Various measurement techniques have been applied which involve direct measurement of in-bore projectile velocity, such as magnetic flux sensors (B-dot probes) [1,2], optical interferometry using velocity interferometer system for any reflecter (VISAR) [3] and photonic Doppler velocimetry (PDV) [4], and Doppler radar [5-7]. However, the B-dot probes technique is limited by the linear density with which the probes can be installed along the length of the launcher as well as the accuracy with which the probes can be calibrated [2], and it is impractical for routine use. Optical interferometer requires specialized equipment and precise setup and calibration to achieve a high temporal and spatial resolution, and this limits its practical industrial application. Doppler radar has been demonstrated on small caliber railguns for velocities up to 1200 m/s [6] and 2000 m/s [5]. Though Doppler radar cannot produce high resolution as Optical interferometry technique, it can be reassembled and amended for extensive test series and is advantageous over other techniques for this flexibility. Recently, a W-band millimeter wave Doppler radar is developed to measure the motion parameters of in-bore projectiles. Compared to the Doppler radar system working at microwave band, the developed millimeter wave radar possesses the merits of smog penetration and higher resolution.

Many researchers have been researching on radar signal analysis for in-bore projectile observation. [8] calculated the projectile velocity by finding the zero crossings of its reflected signal, since the time differences of adjacent zero crossings establish half-wavelengths. However, the resolution of this method is poor when the projectile velocity is low because of the long sine wave periods associated with slow velocity. Also, modern signal processing methods have been employed in motion parameter measurement for in-bore projectile, such as the generalized demodulation, the generalized S-transform, Hilbert transform [9,10]. However, the generalized demodulation and the generalized S-transform method require manual estimation of signal phase [11,12]. When the signal to noise ratio (SNR) is low, the phase estimation error is too large to deteriorate the result of the subsequent motion parameters. Regarding to Hilbert transform method [13], it is based on signal phase computation yet phase unwrapping is not only complicated but also suffers from low SNR.

The developed W-band Doppler radar suffers from lower SNR of in-bore projectile measurement due to a low emission power. To enhance the signal corrupted by noises, time-frequency peak filtering (TFPF) is proposed in [14] and has been proven to be able to accomplish a clean recovery of signals for SNR as low as -9dB. The conventional TFPF exploits a fixed window length for the pseudo Wigner-Ville distribution (PWVD) analysis of nonstationary signals [14,15]. However, a short window length cannot suppress the random noise effectively and a long window length leads to a serious estimation bias and consequently a distortion of the recovered signal. The optimal window lengths should vary with the frequencies of the nonstationary signal. Aiming at improving the shortcomings of conventional TFPF, the ITFPF which determines the optimal window lengths for the nonstationary signal is proposed to achieve a better performance in this paper. And a signal processing method is presented by incorporating ITFPF and digital image processing technique. Here the ITFPF is exploited as a pre-processing step to promise a good performance in low SNR environment, and digital image processing technique is employed to extract the time-frequency ridge. The presented method is focused on the ridge extraction of signal time-frequency representations and it is non-fastidious about the time-frequency distributions.

This paper is organized as follows. Section 2 introduces the developed system for motion parameter measurement and gives the velocity expression of the in-bore projectile. In Section 3, the presented ITFPF for signal pre-processing is described in detail, and the time-frequency ridge extraction method based on curvilinear structure detection and MM is illustrated in Section 4. Section 5 demonstrates the effectiveness and accuracy of the proposed method by processing some of the simulated and experimental data. The last section is the conclusion.

2. **System Description.** The developed W-band radar consists of the antenna, the local oscillator, the circulator, the mixer, the video frequency amplifier, the low-pass filter and the digital signal processing unit. The measurement setup is shown in Figure 1 and it is seen that a reflector is placed in front of the artillery. Also a laser indicator is mounted right beside the radar antenna for alignment, as shown in Figure 2, to make sure that the projectile is illuminated by the radar beam before measuring.

During the system working, the radio frequency signal generated by the local oscillator transmits through the circulator and antenna, and propagates to the reflector placed on the bore axis. Then the signal is reflected to illuminate in the bore. The scattered echo by the projectile propagates back along the same path and is received by the antenna. The received signal is mixed with the local oscillator signal, amplified by the video frequency amplifier and then processed by the digital signal processing unit. And the output

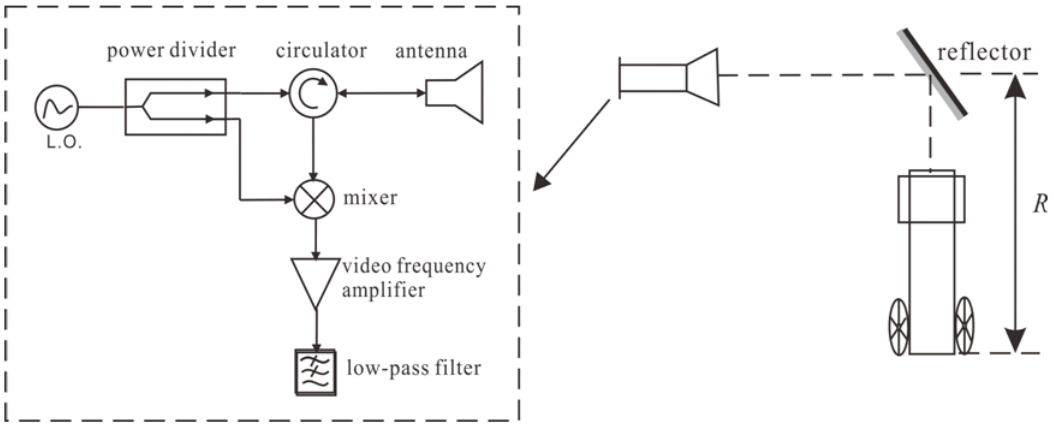

FIGURE 1. Illustration of the developed system measurement setup

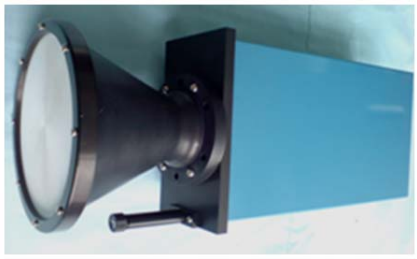

FIGURE 2. Photograph of the radar to measure the motion parameters of in-bore projectile

intermediate frequency signal can be expressed as

$$S_f(t) = A_f \cos\left[2\pi\left(\int f_d(t)dt - \frac{2f_0R_0}{c}\right)\right], \tag{1}$$

where A_f is the amplitude, f_0 is the working frequency of radar, R_0 is the initial range between the projectile and radar, c is the speed of light, $f_d(t)$ is the Doppler frequency caused by the motion of the projectile and can be calculated as

$$f_d(t) = \frac{2f_0}{c}v_r(t), \tag{2}$$

where $v_r(t)$ is the velocity of projectile. Due to the wave propagation mode in bore, the final projectile velocity $v_p(t)$ should multiply $v_r(t)$ by a correction factor of M_c [7], and thus

$$v_p(t) = M_c \cdot v_r(t) = M_c \cdot \frac{cf_d(t)}{2f_0}, \tag{3}$$

where

$$M_c = \frac{1}{\sqrt{1 - \left(\dfrac{1.841 \times c}{\pi \times d \times f_0}\right)^2}} \tag{4}$$

and d is the diameter of the barrel bore.

To achieve $v_p(t)$ from signal $S_f(t)$, a new method is proposed by incorporating the ITFPF method and digital image processing technique. The algorithm is stepped as:

(1) Use the presented ITFPF to reduce noise of the original measurement signal and get the two-dimensional time-frequency representation of the de-noised signal via time-frequency analysis. The ITFPF principle and implementation steps are introduced in Section 3.

(2) Extract the ridge structure of the signal time-frequency representation with the proposed ridge detection method based on gradient determination. Then the detected ridge outline is optimized to get the ultimate time-frequency ridge with MM operators. This is described in detail in Section 4.

(3) Fit the time-frequency ridge data by least square fitting technique and estimate the signal IF with a polynomial function.

Then the velocity of projectile in-bore can be calculated through Equation (3) once the signal IF has been estimated. Correspondingly, the acceleration and travelled distance of the projectile can be deduced by derivation and integration respectively.

3. **Improved Time-Frequency Peak Filtering.** Conventional TFPF reconstructs the signals submerged in additive noise by encoding the noisy signal as IF of a frequency modulated analytic signal with constant amplitude. IF estimation of encoded analytic signal is then performed using the peak of PWVD to restore signal. However, the proper window length selection of PWVD is crucial for the bias of IF estimation increases with the window length and variance decreases. Due to the optimum window length resulting in excellent time-frequency distribution concentration, we present an ITFPF method that determines the best window length of TFPF based on the measure for distributions concentration. For the complex signals, some measures of the ratio of distribution norm, entropy, and distribution energy that all based on the distribution norms are employed [16-18]. Here the concentration measure criterion proposed in [16] is adopted:

$$M[P_x] = \left(\sum_{n=1}^{N} \sum_{k=1}^{K} |P_x(n,k)|^{1/p} \right)^p \tag{5}$$

where $P_x(n,k)$ denotes the discrete time-frequency representation of the signal $x(n)$, and $\sum_{n=1}^{N} \sum_{k=1}^{K} P_x(n,k) = 1$ being the normalized unbiased energy constraint, and $p > 1$. In reality, there is no sharp edge between zero and non-zero elements of the signal time-frequency representation, so the value of $M[P_x]$ could be sensitive to small values of $P_x(n,k)$ for a large p. The robustness may be achieved by using lower-order forms with $p = 2$ or 4 [17]. In this paper, p is set to be 2.

1) Using frequency modulation to encode the original noisy signal. In practice, the signal is modelled to be corrupted by additive noise:

$$x(t) = s(t) + n(t), \tag{6}$$

where $s(t)$ is signal, and $n(t)$ is the additive noise. Encode signal $x(t)$ via frequency modulation as

$$z_x(t) = e^{j2\pi\mu \int_{-\infty}^{t} x(\lambda)d\lambda} = z_s(t) z_n(t), \tag{7}$$

where $z_s(t) = e^{j2\pi\mu \int_{-\infty}^{t} s(\lambda)d\lambda}$, $z_n(t) = e^{j2\pi\mu \int_{-\infty}^{t} n(\lambda)d\lambda}$, and μ is a scale parameter similar to the frequency modulation index. Through this transformation, the additive noise turns into a multiplicative noise, and the IF of signal $z_s(t)$ is $s(t)$. So the signal $s(t)$ can be recovered by estimating IF of signal $z_x(t)$.

2) Assuming that $z_x(nT)$ is a discrete version of the continuous encoded signal $z_x(t)$, then the WVD with a rectangular window $\omega_h(nT) = T/h \cdot \omega(nT/h)$ for the window width

of h can be calculated by

$$P_{z_x}(t,\omega) = \sum_{n=-\infty}^{n=\infty} \omega_h(nT) z_x(t+nT) z_x^*(t-nT) e^{-j2\omega nT}, \tag{8}$$

where $\omega_h(nT) = T/h \cdot \omega(nT/h)$ and $\omega(t)$ is a real-valued symmetric window, T is the sampling interval. To determine the optimum window length from a wide region of possible values, the steepest descend approach is employed. The iteration procedures can be described as

$$h_{m+1} = h_m - \mu_h \frac{M[P_{z_x}; h_m] - M[P_{z_x}; h_{m-1}]}{h_m - h_{m-1}}, \tag{9}$$

where $M[P_{z_x}; h_m]$ denotes the concentration measure of WVD distribution with the window length h_m of the encoded signal $z_x(nT)$, μ_h is the step. The item $\frac{M[P_{zx};h_m]-M[P_{zx};h_{m-1}]}{h_m-h_{m-1}}$ in Equation (9) is implemented to calculate the gradient $\partial M[P_{z_x}]/\partial h$. The initial window lengths are small values and the above iterations start from a low-concentrated distribution to the maximally concentrated one which has a minimum concentration measure with the increment of window length. The optimum window length is acquired when the error between h_m and h_{m-1} is less than a set value as the $M[P_{z_x}; h_m]$ reaches to the minimum and thus the gradient $\partial M[P_{z_x}]/\partial h$ is close to 0. In this paper, the algorithm is stopped when $|h_m - h_{m-1}| < 2$.

3) Estimate the peak of PWVD with the optimum window length to restore signal $s(t)$. The original signal $s(t)$ can be recovered by

$$\hat{s}(t) = \hat{\omega}_{z_s}(t) = \frac{\arg\max_\omega [P_{z_x}(t,\omega)]}{\mu} \tag{10}$$

To improve the estimation of motion parameters for in-bore projectile in extremely low SNR, the iterative ITFPF algorithm is applied in which the ITFPF process is repeated on the estimated signal until a satisfied estimation is achieved. The iteration number in the paper is selected as three by experience.

4. **Time-Frequency Ridge Extraction with Image Processing Technique.** The ridge of non-stationary signal time-frequency representation depicts the energy concentration and frequency variation over time. It is often extracted to estimate the IF of components for signal classification and recognition. The two-dimensional representation of a signal in the joint time-frequency domain has led to the use of digital image processing techniques to extract IF. [19] presented a local peak detection and component linking method for estimating the IF of newborn electroencephalography (EEG) signals. Terrien et al. applied active contours or snake algorithms to the analysis of uterine electromyogram signal during gestation in monkeys [20]. As regarding to this paper for in-bore projectile motion parameter measurement, a novel ridge extraction method is proposed based on the idea of curvilinear structure detection [21]. The gradient of every pixel of the time-frequency representation image is calculated to determine whether it is the candidate of the ridges. If so, the position and orientation of the pixel are recorded. The gradient is calculated through the first derivative.

Suppose the time-frequency representation of the signal is

$$z = P(t,\omega), \tag{11}$$

and the gradient of z is correspondingly

$$z' = P'(t,\omega). \tag{12}$$

In the discrete case, the difference between the pixel value and that of the adjacent pixel could be considered as the gradient. To achieve an all-around result, pixels in the neighbour are taken into account. In this paper, a region of 5×5 is chosen to calculate the gradient of every pixel, which is also conducive to noise reduction.

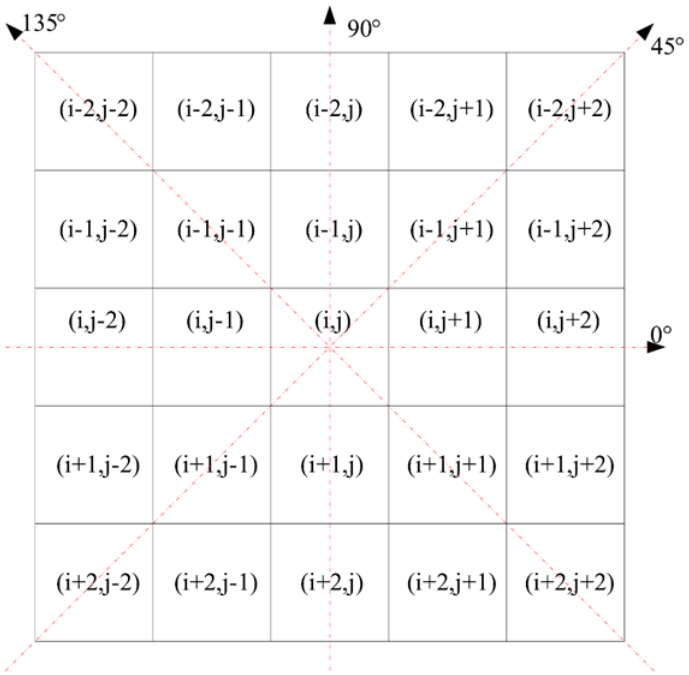

FIGURE 3. Illustration of a 5×5 region for gradient calculation

Figure 3 illustrates a 5×5 region for gradient calculation. As is shown, the gradient values of every pixel (i, j) of the time-frequency representation image are calculated along 0°, 45°, 90° and 135° direction respectively, of which the maximum is taken as the final gradient value. Specific to 90° direction for example, the gradient of pixel (i, j) is calculated as:

$$G_{90} = \lambda_1 F_1 + \lambda_2 F_2 + \lambda_3 F_3 + \lambda_4 F_4, \tag{13}$$

where λ_p $(p = 1, 2, 3, 4)$ is the weight factor, and F_q $(q = 1, 2, 3, 4)$ is defined as:

$$\begin{aligned}
F_1 &= f(i-1,j) - f(i,j), \\
&\quad \text{if } f(i,j) < f(i-1,j) \\
F_2 &= f(i+1,j) - f(i,j), \\
&\quad \text{if } f(i,j) < f(i+1,j) \\
F_3 &= [0.3f(i-2,j-1) + 0.4f(i-2,j) + 0.3f(i-2,j+1)] - f(i-1,j), \\
&\quad \text{if } f(i-1,j) < [0.3f(i-2,j-1) + 0.4f(i-2,j) + 0.3f(i-2,j+1)] \\
F_4 &= [0.3f(i+2,j-1) + 0.4f(i+2,j) + 0.3f(i+2,j+1)] - f(i+1,j), \\
&\quad \text{if } f(i+1,j) < [0.3f(i+2,j-1) + 0.4f(i+2,j) + 0.3f(i+2,j+1)]
\end{aligned} \tag{14}$$

Gradients along other directions can be achieved similarly and the maximum of the four is selected as the final gradient value.

$$G_{\max} = \max(G_0, G_{45}, G_{90}, G_{135}) \tag{15}$$

If $G_{\max}$ is greater than a predetermined threshold G_t, then the pixel (i, j) is marked as a successful candidate point and the time-frequency ridge structure which has a sort

of "width" is obtained. The threshold G_t could be a global constant or an adaptive local variable for specific time-frequency representation image. The global threshold is adopted in this paper to simplify analysis.

After that, MM method [22] is employed to deal with the geometry of the image to get a thinned ridge. Its primary idea is to collect image information with a structure element, carrying shape, size, gradation, chroma and other information – when the structure element is moving continuously in the image, the interrelation of various parts in the image can be examined to obtain structure characteristics. As the velocity of projectile varies increasingly with time in the bore, the IF of Doppler radar signal also changes with time and is commonly depicted with a polynomial function of the time. Lastly, the least square fitting technique is employed to fit the extracted ridge data and the IF estimation is realized to extract the velocity profile.

5. **Results.**

5.1. **Simulation results.** To assess performance of the proposed algorithm, a cosine signal with the third order polynomial phase is considered as radar output in simulation.

$$S_f(t) = \cos\left[2\pi\left(b_0 + b_1 t + b_2 t^2 + b_3 t^3\right)\right]. \tag{16}$$

The signal of length $N = 1024$ in this performance assessment has a sampling frequency of $f_s = 1000$Hz, phase function coefficients of $b_0 = 20$, $b_1 = 568$, $b_2 = -754$, and $b_3 = 502$. White Gaussian noise (WGN) was then added to obtain noisy signal with SNR = 0dB. The noisy signal is preprocessed by TFPF of 3 times iteration first and the de-noisy signal is then analyzed with PWVD and the attained signal time-frequency grayscale image is shown in Figure 4. Then the proposed curvilinear structure detection method and MM are applied to the two-dimensional grayscale image, and the optimized ridge structure is extracted as shown in Figure 5. Then the extracted ridge data is fitted with a polynomial function using least square fitting to realize IF estimation. As can be seen from Figure 6, the estimated IF of simulated signal is quite close to the formula IF.

To evaluate the proposed algorithm performance, noisy signals are obtained with SNRs in the range of 10dB down to −10dB with the step of 2dB. And Monte Carlo simulation with 100 realizations is employed for each SNR. The calculated mean square error (MSE)

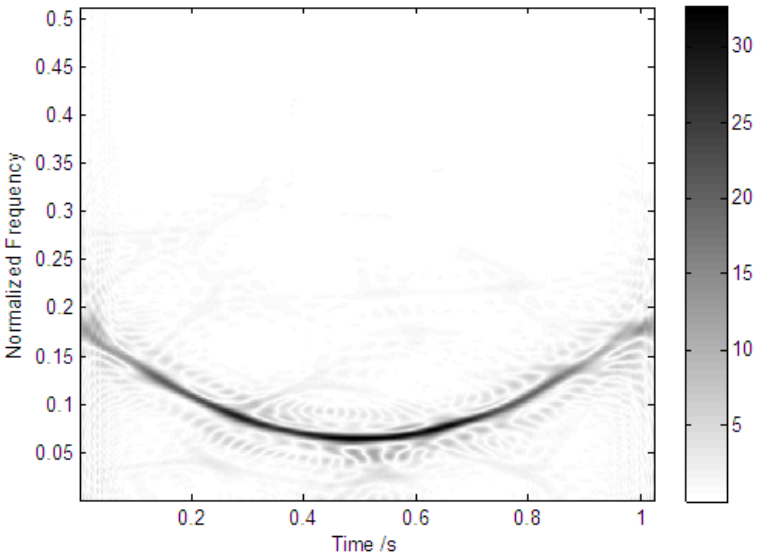

FIGURE 4. The de-noised signal time-frequency representation

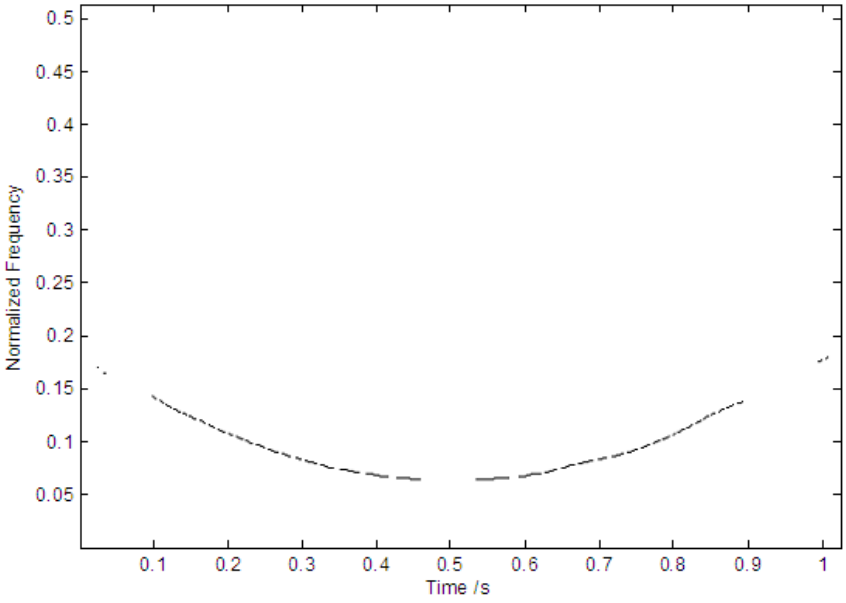

FIGURE 5. Extracted ridge of signal time-frequency representation

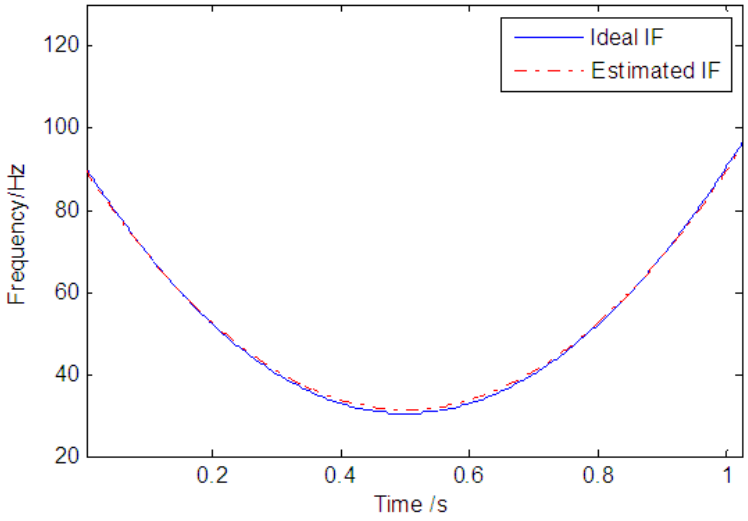

FIGURE 6. Estimated IF of simulated signal compared with ideal IF

is given in Figure 7. Also, the results without pre-processing and with conventional TFPF are given for comparison.

From Figure 7, it is seen that the algorithm breaks down and fails to extract the true ridge of signal time-frequency representation for lower SNR than -2dB without pre-processing, while the algorithms still work well with both TFPF and ITFPF pre-processing applied even when SNR is low down to -10dB. Also the MSEs of ITFPF are about 2.7dB smaller than that of TFPF. It means that the proposed ITFPF has a better ability to improve SNR compared to the conventional TFPF.

The computational complexity of the algorithm is mainly considered in the first two stages. As the most complex part of the ITFPF pre-processing and time-frequency representation of the de-noised signal is PWVD, its computational burden is discussed. Given the discrete implementation of PWVD with data length of N and the window length of N_W, there are $2NN_W(2 + \log_2 2N_W)$ complex multiply operations and $4NN_W \log_2 2N_W$

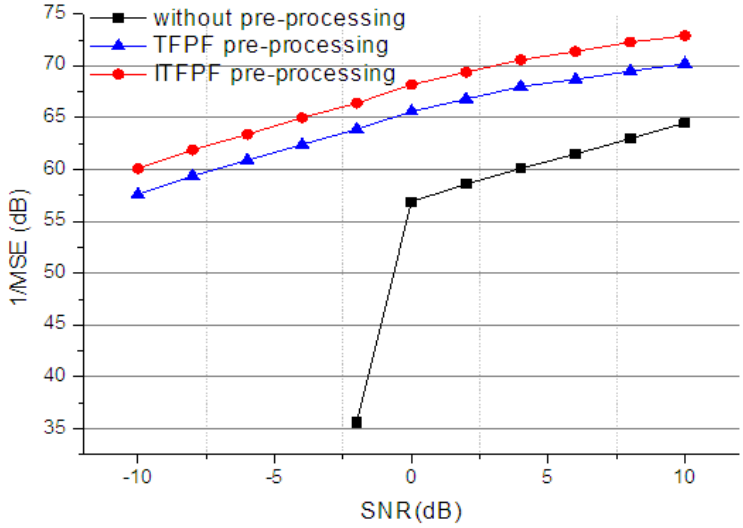

FIGURE 7. MSE results from Monte Carlo simulations for IF estimation

complex add operations needed for the algorithm. For a signal time-frequency image of N_p pixels, the ridge structure detection in the image processing stage costs about $52N_p$ multiply operations and $44N_p$ add operations.

5.2. **Experimental results.** Also to verify the proposed method for in-bore motion parameter measurement application, a group of pyrotechnic propelled 152mm howitzer projectile experimental data is acquired. The shape of the front of projectile is ogival and the W-band Doppler radar working center frequency is 94.3GHz, and the acquired signal in time domain is presented in Figure 8.

Due to the large experimental data length, the acquired signal is divided into several pieces by similar processing procedure as simulation to avoid extremely high computer memory requirement. Then the individually processed result is linked together to form a final ridge. The IF is estimated by fitting the ridge data with a polynomial function using least square fitting. As presented in Figure 9, the estimated velocity profile is obtained

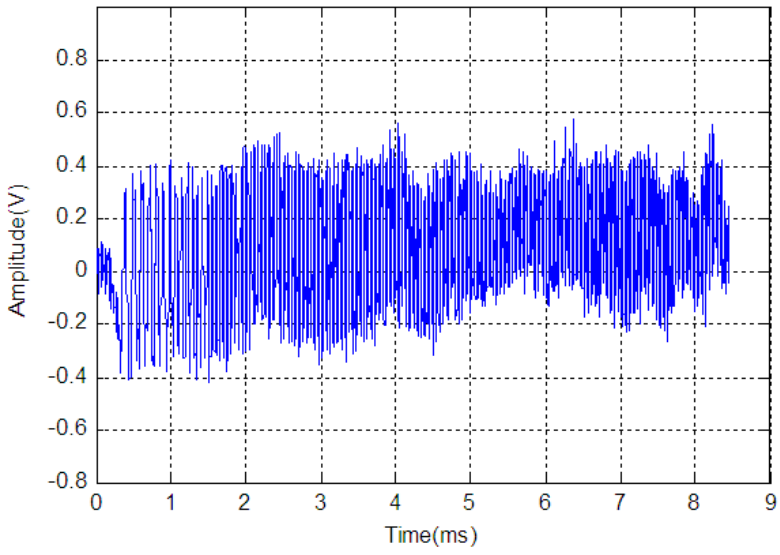

FIGURE 8. The acquired experimental data

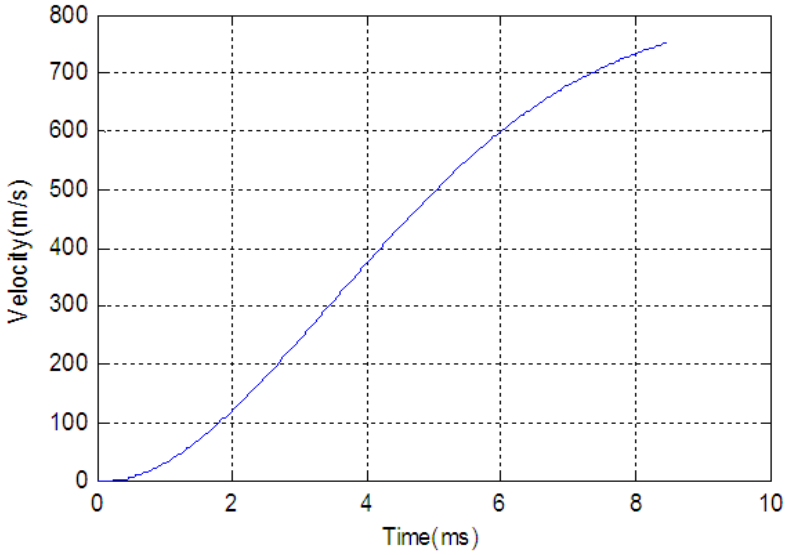

FIGURE 9. Extracted velocity profile of the in-bore projectile

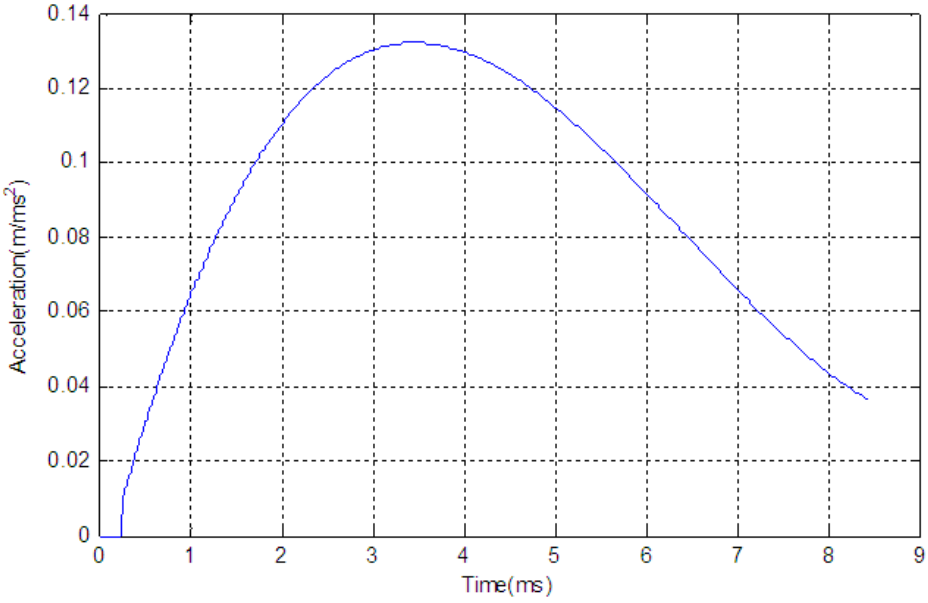

FIGURE 10. Calculated acceleration profile of the in-bore projectile

with Equation (3). Also the acceleration and position profiles over time are deduced and shown in Figure 10 and Figure 11, respectively.

The results show that the velocity of the in-bore projectile is up to maximum 751m/s, also muzzle velocity, at around 8.45ms. The total travelled length of projectile in this experiment is approximately 3.23 meters. Compared with the physical measurement length 3.3 meters taken before the shot, the error of 0.07m can demonstrate the accuracy of the algorithm.

6. **Conclusion.** In this paper, a method incorporating ITFPF and digital image processing technique is proposed to process the signal of projectile in-bore. The pre-processing of iterative ITFPF effectively reduces noise and greatly enhances the signal even in low SNR. Then the two-dimensional signal time-frequency representation of the de-noised signal is obtained via time-frequency analysis for ridge extraction with image processing

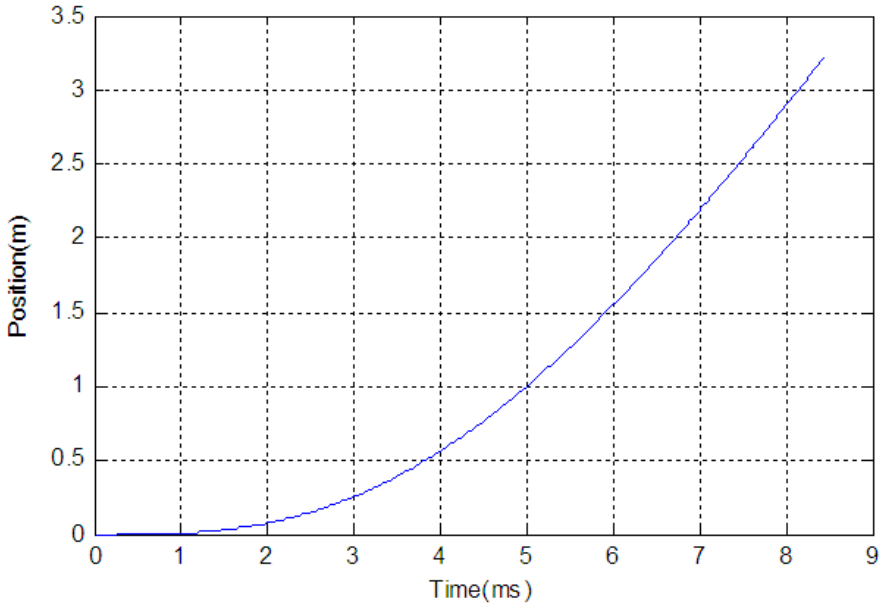

FIGURE 11. Calculated position profile of the in-bore projectile

technique. The curvilinear structure is successfully detected by the proposed algorithm and then the thin time-frequency ridge is obtained through MM. Finally, the IF of the signal is estimated by least square fitting with a low order polynomial function, which correspondingly realizes the motion parameter measurement of the projectile in-bore. Simulation and experiment results show the proposed method can accurately estimate the projectile's relevant motion parameters in-bore, and verify the effectiveness of this method.

As the time-frequency ridge extraction is implemented by image processing, the motion parameter estimation of the projectile in-bore is achieved automatically and rapidly. Human intervention that exists in some other methods is NOT required in this procedure. However, a threshold is set artificially as regarding to the procedure of curvilinear structure detection, which determines the width of curvilinear structure. Further research will focus on threshold selection of the gradient time-frequency representation to ensure extracting a more accurate time-frequency ridge line.

Acknowledgment. This work is partially supported by the National Natural Science Foundation of China (No. 61301213, No. 61501234), and the Natural Science Foundation of Jiangsu Province (No. SBK20130768). The authors also gratefully acknowledge the helpful comments and suggestions of the reviewers, which have improved the presentation.

REFERENCES

[1] Z. Wang, J. He, S. Xia, Z. Xiao, L. Chen, Z. Cheng, M. Dong, J. Li and P. Yan, Evaluation of solid armature's in-bore position, velocity and current distribution using B-Dot probes in railgun experiments, *IEEE Trans. Magnetics*, vol.45, no.1, pp.485-489, 2009.

[2] J. V. Parker, Magnetic probe diagnostics for railgun plasma armatures, *IEEE Trans. Plasma Science*, vol.17, no.3, pp.487-500, 1989.

[3] J. R. Asay, C. H. Konrad, C. A. Hall, M. Shahinpoor and R. Hickman, Continuous measurements of in-bore projectile velocity, *IEEE Trans. Magnetics*, vol.25, no.1, pp.46-51, 1989.

[4] S. J. Levinson and S. Satapathy, High-resolution projectile velocity and acceleration measurement using photinic Doppler velocimetry, *Proc. of the American Physical Society Topical Group on Shock Compression of Condensed Matter*, pp.585-588, 2009.

[5] M. Seth and Z. R. Raul, Application of W-band Doppler radar to railgun velocity measurements, *Procedia Engineering*, vol.58, pp.369-376, 2013.
[6] M. Schneider, D. Eckenfels and S. Nezirevic, Doppler-radar: A possibility to monitor projectile dynamics in railguns, *IEEE Trans. Magnetics*, vol.39, no.1, pp.183-187, 2003.
[7] S. H. Ong and A. Z. Kouzani, A wavelet-based ammunition Doppler radar system, *Lecture Notes in Computer Science*, vol.2251, pp.382-392, 2001.
[8] J. Justiss, S. Levinson and R. Russell, Microwave Doppler measurements of projectile velocity in a single-stage GAS gun, *A714914*, 2004.
[9] C. Bai, Z. L. Xiao and J. Z. Xu, Time-frequency denoising method based on generalized demodulation and generalized S-transform, *Journal of Detection Control*, vol.33, no.4, pp.28-33, 2011.
[10] J. Xiao, B. Liu, Y. L. Guo and W. Kong, Signal processing of microwave interferometer based on Hilbert transform, *Journal of Detection & Control*, vol.32, no.1, pp.80-83, 2010.
[11] J. S. Cheng, Y. Yu and D. J. Yu, The envelope order spectrum based on generalized demodulation time-frequency analysis and its application to gear fault diagnosis, *Mechanical Systems and Signal Processing*, vol.24, no.2, pp.508-521, 2010.
[12] M. D. Adams, K. Faouzi and K. W. Rabab, Generalized S transform, *IEEE Trans. Signal Processing*, vol.50, no.11, pp.2831-2842, 2002.
[13] N. E. Huang and S. S. Samuel, *Hilbert-Huang Transform and Its Applications*, World Scientific, Singapore, 2005.
[14] B. Boashash and M. Mesbah, Signal enhancement by time-frequency peak filtering, *IEEE Trans. Signal Processing*, vol.52, no.4, pp.929-937, 2004.
[15] V. Ivanovi, M. Dakovi and L. Stankovi, Performance of quadratic time-frequency distributions as instantaneous frequency estimators, *IEEE Trans. Signal Processing*, vol.51, no.1, pp.77-89, 2003.
[16] L. Stankovic, A measure of some time-frequency distributions concentration, *Signal Processing*, vol.81, no.3, pp.621-631, 2001.
[17] V. Sucic, N. Saulig and B. Boashash, Estimating the number of components of a multicomponent nonstationary signal using the short-term time-frequency Rényi entropy, *EURASIP Journal on Advances in Signal Processing 2011*, no.1, pp.1-11, 2011.
[18] V. Sucic, N. Saulig and B. Boashash, Analysis of local time-frequency entropy features for nonstationary signal components time supports detection, *Digital Signal Processing*, vol.34, pp.56-66, 2014.
[19] L. Rankine, M. Mesbah and B. Boashash, IF estimation for multicomponent signals using image processing techniques in the time-frequency domain, *Signal Processing*, vol.87, no.6, pp.1234-1250, 2007.
[20] J. Terrien, C. Marque and G. Germain, Ridge extraction from the time-frequency representation (TFR) of signals based on an image processing approach: Application to the analysis of uterine electromyogram AR TFR, *IEEE Trans. Biomedical Engineering*, vol.55, no.5, pp.1496-1503, 2008.
[21] B. Obara, F. Mark, G. David and G. Vicente, Contrast-independent curvilinear structure detection in biomedical images, *IEEE Trans. Image Processing*, vol.21, no.5, pp.2572-2581, 2012.
[22] L. Najman and H. Talbot, *Mathematical Morphology*, John Wiley & Sons, Inc., New York, 2013.